Machine learning-assisted finite element modeling of additively manufactured meta-materials

Meynen, Alexander; Kolken, H. M.A.; Mulier, Michiel; Zadpoor, Amir A.; Scheys, Lennart

DOI
10.1186/s41205-025-00286-7

Publication date
2025

Document Version
Final published version

Published in
3D Printing in Medicine

3D Printing in Medicine

RESEARCH

Open Access

Machine learning-assisted finite element modeling of additively manufactured meta-materials

Alexander Meynen[1*], HMA Kolken[2], Michiel Mulier[1,3], Amir A. Zadpoor[2] and Lennart Scheys[1,3]

Abstract

Mechanical characterization of three-dimensional (3D) printed meta-biomaterials is rapidly becoming a crucial step in the development of novel medical device concepts, including those used in functionally graded implants for orthopedic applications. Finite element simulations are a valid, FDA-acknowledged alternative to experimental tests, which are time-consuming, expensive, and labor-intensive. However, when applied to 3D-printed meta-biomaterials, state-of-the-art finite element modeling approaches are becoming increasingly complex, while their accuracy remains limited. A critical condition for accurate simulation results is the identification of correct modelling parameters. This study proposes a machine learning-based strategy for identifying model parameters, including material properties and model boundary conditions, to enable accurate simulations of macro-scale mechanical behavior. To achieve this goal, a physics-informed artificial neural network model (PIANN) was developed and trained using data generated through a fully automated finite element modeling workflow. Subsequently, the PIANN model was then tested using real experimental force-displacement data as its input. The experimental data from 3D-printed structures were used to predict the associated parameters for finite element modeling. Finally, the workflow was validated by qualitatively and quantitatively comparing simulation results to the experimental data. Based on these results, we concluded that the proposed workflow could identify model parameters such that the predictions of associated finite element simulations are in agreement with experimental observations. Furthermore, resulting finite element models were found to outperform state-of-the-art models in terms of both quantitative and qualitative accuracy. Therefore, the proposed strategy has the potential to facilitate the broader application of finite element simulations in evaluating 3D-printed parts, in general, and 3D-printed meta-biomaterials, in particular.

Keywords 3D printing, Finite element simulation, Functionally graded implant, Machine learning, Physics-informed artificial neural network

*Correspondence:
Alexander Meynen
alexander.meynen@kuleuven.be
[1]Institute for Orthopaedic Research and Training (IORT), KU Leuven, Leuven, Belgium
[2]Department of Biomechanical Engineering, Delft University of Technology, Delft, Netherlands
[3]Division of Orthopaedics, University Hospitals Leuven, Leuven, Belgium

Introduction

Three-dimensional (3D) printing offers immense design freedom compared to conventional manufacturing techniques, enabling the design of parts with complex geometries in a wide range of materials and across various industries. Metal 3D printing is gaining popularity, particularly in areas where this design freedom can be leveraged to create parts that offer superior performance and unique functional properties. One of the first applications in orthopedics was the fabrication of fully personalized implants for the treatment of complex skeletal pathologies, where off-the-shelf implants can often not provide adequate solutions [1, 2]. More recently, the concept of meta-biomaterials has emerged, leading to the development of porous biomaterials with unusual combinations of mechanical, mass transport, and biological properties, which can enhance the performance of orthopedic (regenerative) implants [3, 4]. In such designer biomaterials, the micro-architecture of the lattice structure, its relative density, porosity, pore size, and the chosen material type can all be adjusted to achieve favorable macroscale properties. Several potential concepts using these materials have already been proposed in the literature, indicating the potential of meta-biomaterials to improve implant fixation and bony in-growth, thereby improving implant longevity [3, 5, 6].

However, bringing these concepts from bench to bedside is challenging and requires the accurate characterization and optimization of their mechanical performance. Characterization of 3D printed lattice structures through experimental testing is, however, time-consuming, expensive, and laborious [7]. The fact that the parameters of the 3D printing process, such as powder bed fusion (PBF), can influence the geometry of the struts and the effective compressive properties of the resulting meta-biomaterials further complicates this process. Indeed, these variables, including laser scanning speed, laser power, build direction, the (flow) properties of the metal powder, and layer thickness, all affect the microscale geometry of lattice structures in terms of their strut thickness variability, strut waviness, unfused powder particles, and porosities [8–11]. In silico approaches, especially finite element (FE) modeling, offer a cheaper and more efficient alternative to experimental testing for such purposes [12–14]. Recently, researchers have created FE models that aim to replicate the experimental testing conditions and the as-manufactured specimen geometries as closely as possible. However, model improvements significantly complicate the creation of FE models and often require costly imaging modalities, such as micro-CT scanners, which complicates their application [15].

As an intermediate solution, many studies suggest a heuristic approach to determine at least some of the modelling parameters, such as friction coefficients, which are difficult to determine experimentally. This process of inverse parameter identification, however, is time-consuming. While semi-automatic parameter optimization algorithms can be used for this purpose, the success of these algorithms is highly dependent on their initialization point. Given that the best initialization points are typically unknown, such processes require expert knowledge to obtain acceptable results [16]. Furthermore, if the parameters of the 3D printing process or the base material are changed, the process of parameter tuning is identified all over again [17].

An alternative solution for identifying the parameters of in silico models is to utilize machine learning (ML) approaches. Here, an ML model is trained and subsequently used to predict modeling parameters of FE models based on the mechanical response of a structure as input. The ML model thus provides a nonlinear mapping from the mechanical response space to the space of possible modeling parameters. Artificial neural networks (ANNs), specifically a physics-informed artificial neural network (PIANN) model, are typically well-suited for this type of regression problem. Indeed, these networks have already been used to predict the constitutive behavior of materials [17, 18]. However, none of these studies include all the necessary modelling parameters, such as friction coefficients and boundary conditions.

As a consequence, there is a need for more comprehensive models that enable the integral parameter identification process [17–21]. We, therefore, aimed to develop a strategy that utilizes an ANN model for the direct identification of FE model parameters to simulate the mechanical behavior of 3D printed meta-biomaterials. To achieve this aim, we first developed a semi-automated finite element (FE) modeling workflow to create a library of model-predicted force-displacement curves. Subsequently, we utilized this library to train and validate an artificial neural network (ANN) model. Finally, we validated the proposed approach by applying it to the problem of identifying FE model parameters of highly porous 3D printed meta-biomaterials and comparing the resulting simulation results with experimental data.

Methods

Artificial neural network

ANNs are regularly chosen for their ability to solve nonlinear regression problems [22]. The objective of the implemented ANN was to predict the optimized FE model parameters that yield the best match between simulated and experimentally obtained force-displacement data. While different neural network architectures can be used for regression problems, we employed the most widely applied network architecture: a multilayer perceptron consisting of an input layer, one or more hidden

layers, and an output layer (Fig. 1). Each layer, except for the input layer, consisted of nodes (= neurons) working with nonlinear activation functions. Each of these nodes is connected to all the nodes of the previous layer, receiving the output of the last layer as input. The number of nodes in the hidden layer is a design variable of the PIANN. While a high number of hidden neurons allows for capturing complex relationships between the input and output spaces, it could also lead to overfitting of the PIANN to the training data. The network architecture and its training parameters were, therefore, defined using several hyperparameters. The effects of these hyperparameters on the performance of the PIANN were then systematically studied in a 4-fold cross-validation study. The parameters studied included the number of nodes in the hidden layers, the number of training epochs, and the batch size used to train the network. A total of 1350 parameter combinations were considered (Table 2). The network architecture was implemented using Keras version 2.5.0, with cross-validation performed with Scikit-learn version 0.24 [23, 24]. The hyperparameter optimization process resulted in a network with three hidden layers, whose neurons were activated by rectified linear unit (ReLU) activation functions.

The training of the ANN is the process of tuning the learnable network parameters, consisting of the weights and biases of the activation functions. The goal of the training process is to determine the network parameters that minimize the error between the predicted finite element (FE) model and the actual finite element (FE) parameters for a given force-displacement curve, using a cost function. A mean squared error was chosen as the cost function as it is the most commonly used for regression problems. The optimization of the cost function was performed using the adaptive stochastic gradient descent algorithm, Adam [25]. The number of epochs and batch size used for the final training of the model were already identified in the above-described cross-validation study. The complete dataset was randomly split into a training set (85%) and a validation set (15%) to evaluate the validation error. We did not consider a separate test dataset, since the ANN will be validated using real experimental data.

Additionally, the performance of the ANN was compared to that of two other machine learning models. First, a multi-target support vector regressor (SVR) was implemented. SVRs are a generalization of support vector classifiers for solving regression problems [26]. By design, this algorithm is used for single-target regression problems. Therefore, a multi-regression model consisting of multiple single support vector regressors (SVRs) was implemented. The model employs a radial basis function as its kernel, utilizing regularization. Second, a random forest regression (RFR) model was chosen as an alternative model. RFR models combine multiple regression trees and can be used for multi-target regression problems [27]. An advantage of RFR models is their interpretability and simplicity in comparison to ANNs. In this study, we implemented an RFR model with 100 trees and a maximum tree depth of 30. These model parameters were chosen heuristically and not optimized further.

Finite element model

This section describes the FE model that simulates the compression behavior of 3D-printed meta-biomaterials. Several FE modeling techniques have already been considered and tested to model the behavior of porous lattice structures [28]. To achieve this, we developed a semi-automated workflow utilizing Abaqus Python scripts

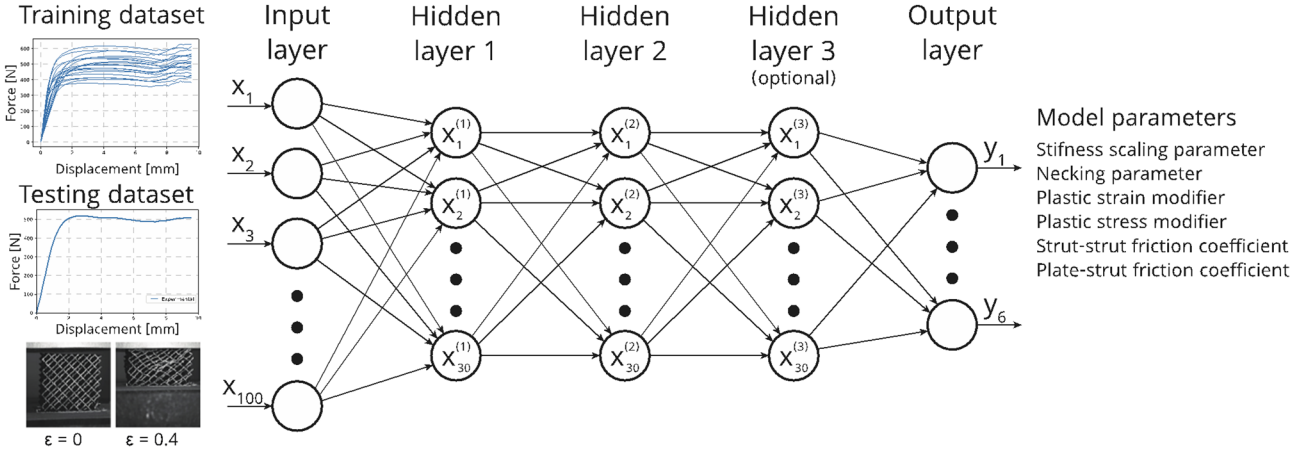

Fig. 1 An overview of the ANN approach used for the estimation of the modelling parameters needed for the FE modeling of 3D printed meta-biomaterials. An ANN model was trained using FE-generated training data to predict the modelling parameters. The performances of ANN architectures with both two and three hidden layers were evaluated. The testing and evaluation of the resulting ANN model were performed using previously unseen simulation data, as well as experimental force-displacement curves measured during compression tests

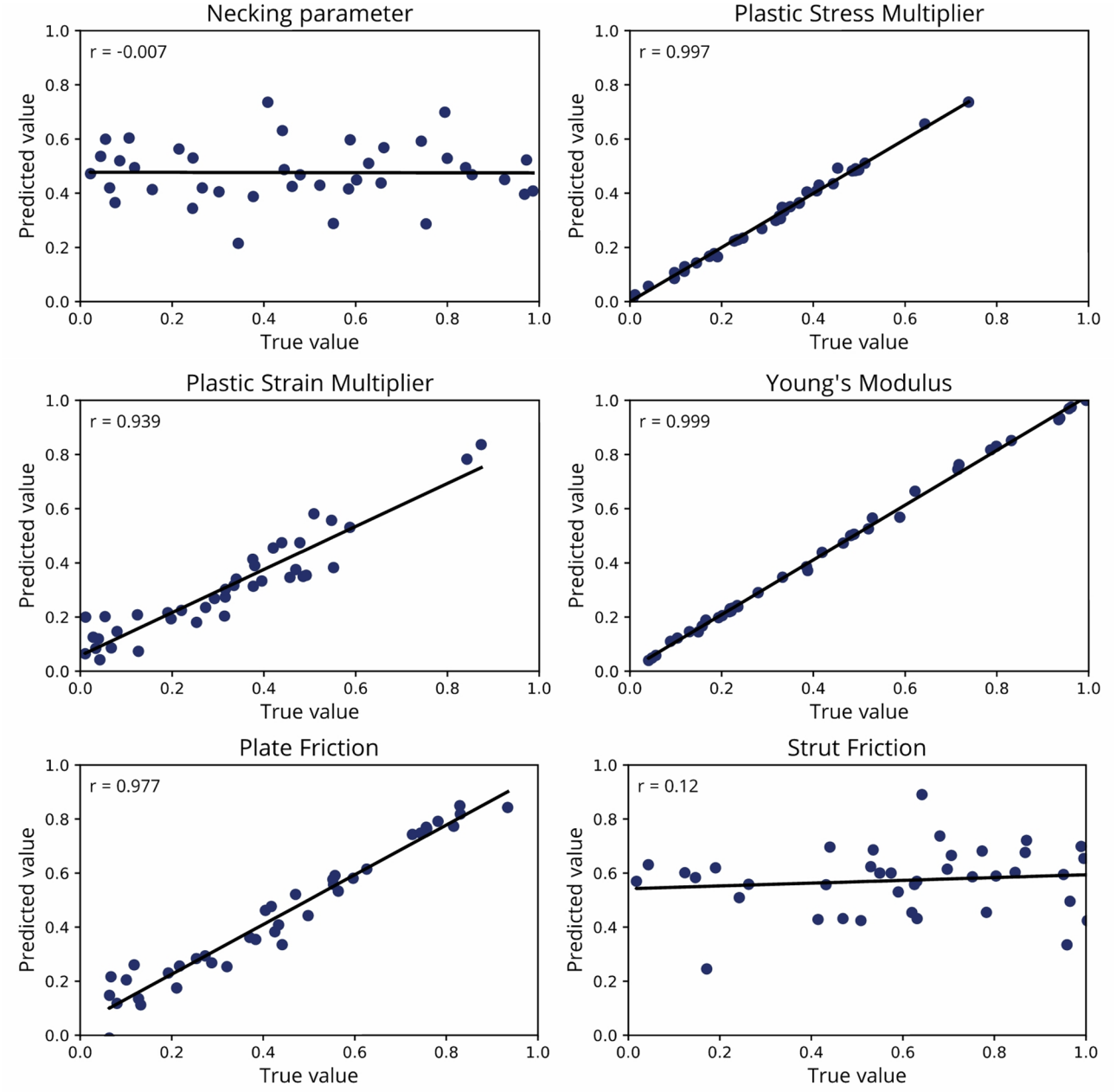

Fig. 2 The scatter plots indicate the actual value vs. the predicted value for each of the model parameters. Whereas the model did not accurately predict the necking and strut friction parameters, the PIANN model accurately predicted all the other parameters. The predictions were most accurate for the Young's modulus, closely followed by the plastic stress multiplier

Table 1 An overview of the range of modelling parameters that were sampled using a Latin hypercube sampling method

Model parameter	Range
Stiffness scaling parameter	40,000–120,000 MPa
Necking parameter	0.5–1.0 x original slope
Plastic stress modifier	0.8–1.4 x original stress magnitude
Plastic strain modifier	0.5–1.1 x original strain magnitude
Strut-Strut friction coefficient	0.1–0.5
Plate-Strut friction coefficient	0.1–0.5

(version 2017, Dassault Systèmes, Vélizy-Villacoublay, France).

The goal of the workflow was to capture the entire experimental process as closely as possible, consisting of both the specimens and the uniaxial compression testing protocol. The starting point of the workflow was the 3D geometry of the specimens. An idealized representation of the as-manufactured sample geometry was modelled in 3D. The average diameter of the strut cross-section was derived from a micro-CT scan, as described in the

Table 2 Five best and worst performing network architectures and training hyperparameters based on the cross-validation study. The values evaluated for each hyperparameter are presented within parentheses

Batch Size	Epochs	# Neurons L1	# Neurons L2	# Neurons L3	MSE
(500,1000,5000)	(250,500,1000)	(64,48,32,24,16)	(64,48,32,24,16)	(48,32,24,12,6)	
1000	500	16	8	48	0,028
500	1000	16	8	0	0,029
1000	500	48	48	6	0,030
1000	500	32	24	6	0,030
500	500	24	8	0	0,031
500	1000	16	48	48	0,064
500	1000	32	48	48	0,064
5000	250	16	24	6	0,066
5000	250	48	48	6	0,071
5000	250	64	8	6	0,080

supplementary document. This geometry was then converted to a FE element mesh, using modified quadratic (C3D10M) elements (Fig. 3a). These elements are preferred over standard quadratic (C3D10) elements in applications with contact scenarios and large strains. Element size was determined based on a mesh convergence study, where the mesh was refined until the change in the peak reaction force was less than 2.5%. Next, the uniaxial compression tester was modelled as two rigid compression plates, which were automatically generated based on the geometry of the underlying lattice structure.

As this study concerns explicitly the behavior of 3D-printed meta-biomaterials fabricated from commercially pure titanium, reference material properties were derived from a uniaxial tensile test of the bulk material performed and provided by the manufacturer, 3D Systems (Leuven, Belgium). The associated force-displacement curve of the bulk material was then parameterized using four parameters, enabling the efficient subsequent variation of the implemented properties. Firstly, Young's modulus variations were modeled using a *stiffness scaling* parameter. Secondly, a 'necking' parameter was implemented to capture variability in softening behavior exhibited by the material when loaded beyond its ultimate strength. Thirdly, a 'plastic stress modifier' was implemented, which adjusts the material's strength in the plastic region. Lastly, a 'plastic strain modifier' adjusted the ductility of the material. These four parameters enable us to alter the constituent relationships of the material and model the associated variability in the deformation behavior of 3D-printed meta-biomaterials. Additional parameter variations include the coefficients of friction between the compression plates and the lattice structure, as well as the friction coefficients between the struts themselves. All models were simulated using the explicit solver of Abaqus. Uniform mass scaling was employed to enhance simulation speed. The mass scaling coefficient was determined based on a preliminary convergence study, ensuring that the kinetic energy was less than 5% of the total energy.

Data generation

The resulting training dataset for the ANN consisted of 250 force-displacement curves from FE simulations with varying model parameters. The modeling parameters for these simulations were chosen using a Latin hypercube sampling method in pyDOE (version 0.3.8). The sample ranges for each parameter were selected empirically (Table 1). Hereafter, the Abaqus input files were automatically generated with the corresponding parameters.

The resulting force-displacement curves were augmented with Gaussian noise data, having a zero mean and a standard deviation of 5. This noise was added to account for some of the randomness in the experimental data, as well as in the metal printing process (i.e., PBF). Both input and output parameters of the ANN were scaled using a min-max scaler to confine all the values to the range between 0 and 1. The scaling of the training and validation data was performed independently of each other.

Validation

Experimental data were available from prior experiments and served as the validation dataset for the PIANN model [5]. During the experiments, four types of diamond-type specimens with a porosity of 98% were compressed, and their force-displacement response was recorded. The mean force-displacement curve from the four samples was calculated and was subsequently introduced as input to the PIANN model. The predicted modelling parameters were then used in an FE simulation, and the simulation results were compared to real experimental data. We compared the mechanical behavior of the structures both quantitatively, by analyzing their force-displacement responses and elastic gradients, and qualitatively, by examining their corresponding deformations at the end of the test against the deformed simulation results.

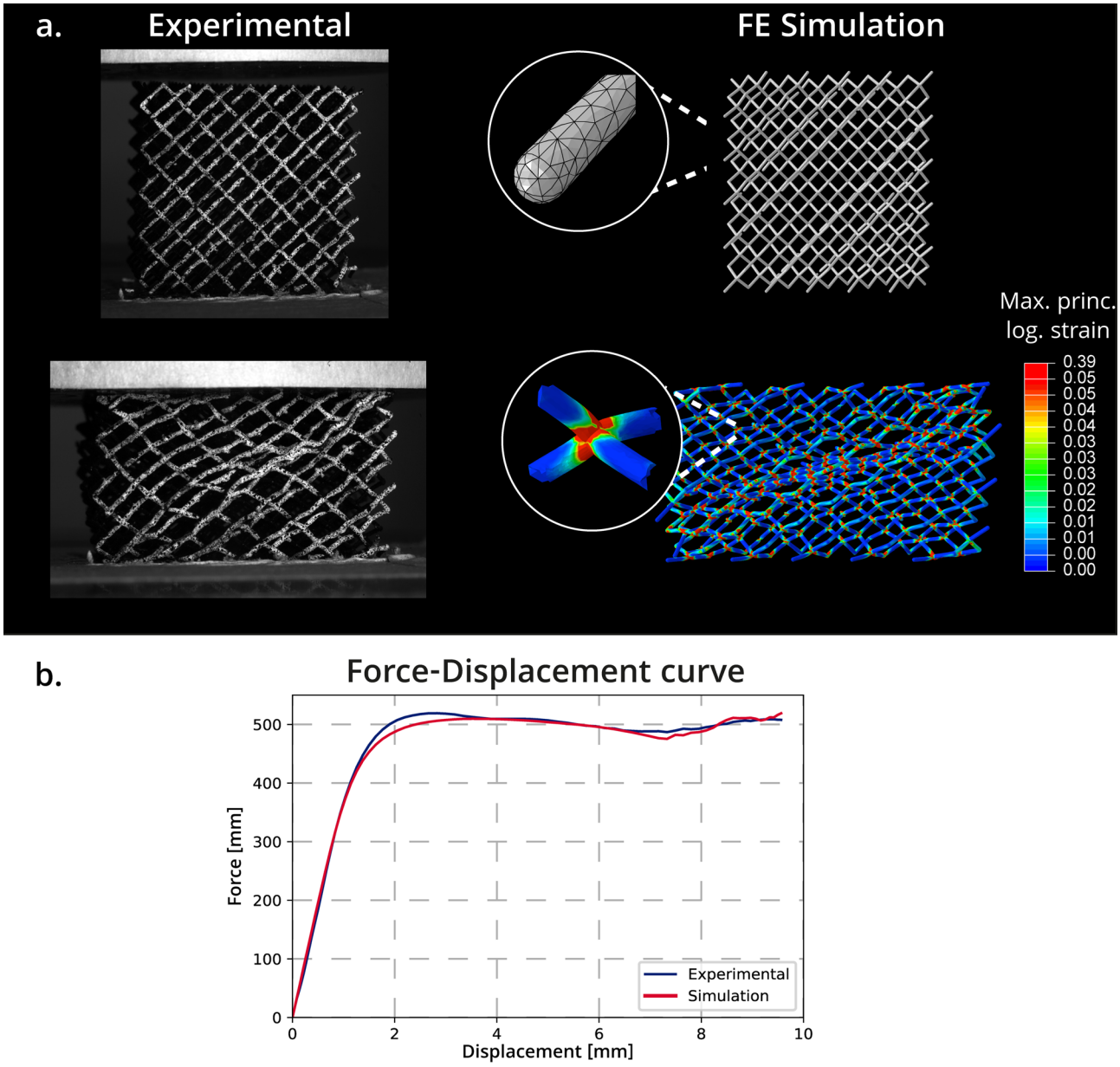

Fig. 3 The experimental data were used to generate an FE model. The deformation behavior of the experimental specimen (**a**) was similar to the behavior observed in the simulations. The maximal strain values were found near the strut connections. The force-displacement curves (**b**) showed almost perfect agreement between the experimental results and the FE simulation

Results

The results of the five best and worst hyperparameter combinations from the 4-fold cross-validation study are presented in Table 2. Subtle differences in accuracy were observed between the different network architectures. Based on these findings, an architecture with three hidden layers (16, 8, and 48) was chosen, and training was performed with a batch size of 1000 samples and 500 training epochs.

The Adam optimizer was found to exhibit good convergence behavior, with both training and validation losses decreasing over the training iterations. The optimized training loss was 2.7%, and the respective validation loss was 3.2%. The PIANN model outperformed the alternative SVR and RFR models for the validation dataset. The root mean square error (RMSE) of the PIANN model was 0.18, whereas the RMSE of the SVR model (0.21) was 14% higher. The RFR was the worst-performing model, with an RMSE of 0.26, representing a 31% increase compared to the prediction error of PIANN.

The accuracy of the predicted model parameters varied between parameters, as shown in Fig. 2. The material necking parameter and strut friction coefficient could not

be accurately predicted by the neural network, as indicated by their respective Pearson's correlation coefficient of -0.007 and 0.12. In contrast, the bulk material properties were predicted accurately by the neural network. The same held for the friction coefficient between the compression plates and the lattice structure. The highest accuracy was found for the Young's moduli ($r = 0.999$).

Figure 3 (a) illustrates the typical deformation of the considered meta-biomaterials, which is characterized by the diagonal collapse of the lattice struts. A qualitatively similar pattern was observed in the simulation results, although a quantitative comparison is challenging due to the geometric complexity before and after testing. The highest maximal principal strain values of 40% were found near the connection points of the struts. The experimental and simulated force-displacement curves are presented in Fig. 3 (b). The simulation data is derived from a model whose parameters were predicted by the PIANN model after being fed the experimental force-displacement curve. The quantitative agreement between both curves was found to be excellent, with a relative error of 2.5% at the point of peak experimental force. The RMSE between both curves was 7.67 N. The simulated elastic gradient was 15.87 MPa, compared to an experimental elastic gradient of 15.78 MPa, yielding an error of 0.6%.

Discussion

We proposed a novel inverse model parameter identification method to accurately simulate the behavior of 3D printed meta-biomaterials based on a single force-displacement curve. Parameter identification was performed using ML models. This approach provides an alternative to trial-and-error-based and optimization-based inverse methods that have been previously proposed in the literature [29]. The main disadvantage of the latter methods is that they require iterative computations to find the best matching parameters. For computationally demanding models, which is the case for 3D printed meta-biomaterials, the associated time cost could significantly limit their potential use [17]. Trial-and-error-based approaches require a high degree of expert knowledge [16, 17, 29]. The presented ML approaches, which are sometimes referred to as direct inverse methods, bypass the computational cost once the dataset for model training is available. The reusable trained model can then predict the optimized model parameters for geometrically similar structures in real-time, without incurring additional computational requirements. Our study demonstrates that this method can effectively identify model parameters of highly porous titanium lattice structures and that the resulting parameters yield accurate simulation results.

Current research efforts aim to develop accurate simulations of the compressive behavior of metallic lattice structures [30]. Many of these approaches require advanced imaging techniques and material testing equipment to obtain the geometry of the specimens [12, 31–33]. Nonetheless, even then, many of these approaches fail to capture the actual mechanical behavior of the specimens, and obtaining accurate simulation results remains a challenge. The documented error in the elastic gradient using these approaches can reach 50% or more, whereas the approach presented in this study achieves an error of less than 1% [7, 15, 33–35]. Furthermore, in the vast majority of the recently validated approaches, the strain range on which the simulations are validated is limited to only a small range (i.e., sub-5% strains), whereas our validation range covers strains of up to 40% [36]. The presented approach prioritizes the accuracy of the macro-behavior over the exact modelling of the micro-scale model parameters. The predicted model parameters are, therefore, of a practical nature, meaning that they compensate for confounding factors, such as strut variability, porosities, or unfused material particles, which are consequently not explicitly captured in our FE model. It should be noted, however, that our approach excludes some application types, such as a detailed analysis of the micro-scale (i.e., sub-strut level) behavior of the meta-biomaterials. In many applications, however, one is interested in the macro-scale behavior of a structure, such as its strength and stiffness. The alternative approach of modeling the part as a solid part based on the experimental force-displacement curve is often unsatisfactory because it does not account for strut failure or the deformation behavior of the structure. In contrast, the proposed methodology still accounts for these aspects and, as such, can be expected to be a more accurate tool to evaluate the macro-scale behavior of porous lattice structures.

Different ML methods can be used to identify modelling parameters directly [37]. Three different ML models were implemented in this study. Among these models, the PIANN model outperformed the others. In addition to this better performance, neural network architectures like this are highly scalable and adaptable to more complex input or output parameters. In this study, we applied the PIANN model to predict the modeling parameters of highly porous metallic lattice structures consisting of diamond unit cells. However, the presented approach is not limited to this specific lattice design. It could be modified with relative ease for application to different unit cell types, porosities, or simulations of different experimental setups. A well-known issue with ANN models is their lack of interpretability. Despite recent efforts, they are still considered "black box" algorithms, especially in deep learning applications [38]. This is indeed where both the

SVR and RFR models are advantageous, as they allow for the calculation of the feature importance, enabling a degree of interpretability.

A notable point of interest is the PIANN model's inability to accurately predict the necking parameter and the strut-strut friction coefficient. While the force-displacement curves derived from the predicted parameters showed near-perfect agreement with experimental data, the individual predictions for these two parameters were poor. This discrepancy suggests either a limited sensitivity of the force-displacement response to variations in these parameters or a potential compensatory relationship between them. In other words, changes in one parameter may be offset by changes in the other, leading to multiple parameter combinations that result in indistinguishable global mechanical behaviour. This could explain the low correlation observed during validation, indicating that the inverse problem may be ill-posed for these specific parameters. Further work is needed to disentangle their contributions, potentially through a sensitivity analysis, to better understand their role in the overall mechanical response.

A critical consideration in the development of our PIANN model was the prevention of overfitting, particularly given the training dataset of 250 samples for predicting six model parameters. Several strategies were employed to mitigate the risk of overfitting. The 4-fold cross-validation study ensured robust model selection, while the training and validation loss curves demonstrate healthy convergence behavior without evidence of overfitting. Data augmentation through the addition of Gaussian noise proved essential for improving model generalization. Many ML algorithms generalize better to unseen data when this step is performed (Wen et al., 2021) and omitting this augmentation leads to inaccurate model predictions, suggesting that the model has overfitted to the clean simulation data. Indeed, for specific regions of the material response, the training dataset will inherently differ from the real dataset. One such example is the 'toe region', a characteristic initial nonlinear portion of the force-displacement curve where the force increases gradually before reaching the linear elastic region. This region is present in experimental data, even when compression experiments are correctly executed, due to factors such as initial contact irregularities and specimen alignment, but is absent in the idealized simulation data. Adding noise to the model-generated training data enabled the model to better generalize to these discrepancies. The close agreement between validation performance on simulation data (RMSE = 0.18) and subsequent performance on real experimental data (2.5% peak force error) provides evidence that the model generalizes well beyond its training domain. However, the modest dataset size remains a limitation, and future work should focus on expanding the training data to enhance model robustness further.

Several additional decisions were made during the development of this approach that might have affected its accuracy or limited its future applicability. First, we chose an FE model consisting of solid continuum elements, based on our previous experiences with beam and solid elements. We found that beam elements were unable to fully capture the mechanical effects of the increased strut thickness near the connection points. Previous studies have proposed adjusting the beam element thickness near the connection points [13, 36]. This thickness adjustment could be included in the PIANN model as a parameter to be identified. Such a PIANN model would enable the use of beams instead of solid continuum elements, thereby reducing the computational burden associated with generating the training dataset. Secondly, the cross-section of the struts in our FE model was approximated using perfect circles. However, it is well-known that these cross-sections of thin struts, as a result of the PBF fabrication process, are better approximated by an ellipse [39]. Also, this ellipse's eccentricity could be included as an additional FE model parameter in the PIANN model. Finally, titanium was modelled using homogeneous elastoplastic material properties without a failure criterion. These properties describe the mechanical behavior of the bulk material from which the meta-biomaterials are made. The application of more advanced constitutive models, such as the Johnson-Cook damage model, would enable a more accurate simulation of the strain hardening and ductile damage phenomena that occur during experimental tests [40–42].

The approach presented in this study can predict modeling parameters that enable the accurate simulation of the mechanical behavior of a specific, highly porous titanium structure. Currently, it is unknown how well this approach generalizes to other lattice configurations. Therefore, future research should aim to expand the developed model with additional training data and model parameters, thereby enabling its application to other types of 3D-printed meta-biomaterials. This includes variations in lattice porosities, unit cell architecture, and bulk materials. Furthermore, the process parameters of the PBF process could also be included in the PIANN model to further improve the accuracy of the predicted modeling parameters.

Conclusion

We developed a novel ML-based model to simulate the mechanical behavior of 3D-printed meta-biomaterials. To achieve this, a PIANN model performing direct parameter optimization was trained using model-generated data. This model could accurately predict the required FE modelling parameters based on experimental

data. The PIANN model was also found to outperform some other commonly used ML-based regressors. The developed model is expandable to account for varying model parameters and lattice configurations. The model was corroborated using experimental data available for highly porous titanium lattice structures, yielding good quantitative and qualitative agreement between the experimental and simulated results. The peak force and elastic gradient were predicted with higher accuracy than comparable studies available in the literature.

Furthermore, excellent visual agreement was obtained for the deformed structure. Taken together, our results suggest that the use of ML-based parameter estimation to model the mechanical behavior of 3D-printed meta-biomaterials has the potential to be a valuable tool for evaluating 3D-printed parts and can facilitate a rational design process using FE modeling. As such, the proposed approach has the potential to increase accessibility to FE modeling of 3D printed products by simplifying model creation and validation, thereby unleashing the potential of these models for more efficient design and testing of 3D printed products across various applications.

Acknowledgements
The research for this paper was financially supported by the PROSPEROS I (2014TC16RFCB046) and PROSPEROS II project (2021TC16RFCB041) funded by the Interreg VA Flanders–The Netherlands program of the EU; A.M. is a SB PhD fellow at FWO (Research Foundation– Flanders) grant no. 1SB3819N. The authors would like to thank Christa de Jonge for her assistance during the collection of the experimental validation data.

Author contributions
A.M. was responsible for the conceptualization, methodology development, data collection, original draft preparation and review of the manuscript. H.M.A.K. contributed in the data collection and editing of the manuscript. M.M., A.A.Z. and L.S. contributed in the conceptualisation, supervision and review of the final manuscript.

Funding
The research for this paper was financially supported by the PROSPEROS project, funded by the Interreg VAFlanders– The Netherlands program, CCI grant no. 2014TC16RFCB046; AM was a SB PhD fellow at FWO (Research Foundation– Flanders) grant no. 1SB3819N.

Data availability
Data is available upon reasonable request to the authors.

Declarations

Competing interests
The authors declare no competing interests.

Received: 6 August 2024 / Accepted: 21 June 2025
Published online: 14 July 2025

References

1. Willemsen K, Nizak R, Noordmans HJ, Castelein RM, Weinans H, Kruyt MC. Challenges in the design and regulatory approval of 3D-printed surgical implants: a two-case series. Lancet Digit Health. 2019;1:e163–71.
2. Mulford JS, Babazadeh S, Mackay N. Three-dimensional printing in orthopaedic surgery: review of current and future applications. ANZ J Surg. 2016;86:648–53.
3. Kolken HMA, Janbaz S, Leeflang A, Lietaert SM, Weinans K, Zadpoor HH. Rationally designed meta-implants: a combination of auxetic and conventional meta-biomaterials. Mater Horiz. 2018;5:28–35.
4. Zadpoor AA. Mechanical meta-materials. Mater Horiz. 2016;3:371–81.
5. Kolken HMA, de Jonge CP, van der Sloten T, Garcia AF, Pouran B, Willemsen K, et al. Additively manufactured space-filling meta-implants. Acta Biomater. 2021;125:345–57.
6. Jeffers J, Arkel RV, Ghouse S, Ray S. Surgical implant [Internet]. 2021 [cited 2022 Jan 28]. Available from: https://patents.google.com/patent/US20210275307A1/en
7. Karamooz Ravari MR, Kadkhodaei M. A computationally efficient modeling approach for predicting mechanical behavior of cellular lattice structures. J Materi Eng Perform. 2015;24:245–52.
8. De Pasquale G, Luceri F, Riccio M. Experimental characterization of SLM and EBM cubic lattice structures for lightweight applications. Exp Mech. 2019;59:469–82.
9. Qiu C, Yue S, Adkins NJE, Ward M, Hassanin H, Lee PD, et al. Influence of processing conditions on strut structure and compressive properties of cellular lattice structures fabricated by selective laser melting. Mater Sci Engineering: A. 2015;628:188–97.
10. Echeta I, Feng X, Dutton B, Leach R, Piano S. Review of defects in lattice structures manufactured by powder bed fusion. Int J Adv Manuf Technol. 2020;106:2649–68.
11. Alaña M, Cutolo A, Probst G, Ruiz de Galarreta S, Van Hooreweder B. Understanding elastic anisotropy in diamond based lattice structures produced by laser powder bed fusion: effect of manufacturing deviations. Mater Design. 2020;195:108971.
12. Campoli G, Borleffs MS, Amin Yavari S, Wauthle R, Weinans H, Zadpoor AA. Mechanical properties of open-cell metallic biomaterials manufactured using additive manufacturing. Mater Design. 2013;49:957–65.
13. Smith M, Guan Z, Cantwell WJ. Finite element modelling of the compressive response of lattice structures manufactured using the selective laser melting technique. Int J Mech Sci. 2013;67:28–41.
14. Food AD. Assessing the Credibility of Computational Modeling and Simulation in Medical Device Submissions. Draft Guidance for Industry and Food and Drug Administration Staff. Food and Drug Administration: Silver Spring, MD, USA. 2021.
15. Lei H, Li C, Meng J, Zhou H, Liu Y, Zhang X, et al. Evaluation of compressive properties of SLM-fabricated multi-layer lattice structures by experimental test and μ-CT-based finite element analysis. Mater Design. 2019;169:107685.
16. Morand L, Helm D. A mixture of experts approach to handle ambiguities in parameter identification problems in material modeling. Comput Mater Sci. 2019;167:85–91.
17. Meißner P, Watschke H, Winter J, Vietor T. Artificial neural Networks-Based material parameter identification for numerical simulations of additively manufactured parts by material extrusion. Polymers. 2020;12:2949.
18. Lefik M, Schrefler BA. Artificial neural network for parameter identifications for an elasto-plastic model of superconducting cable under Cyclic loading. Comput Struct. 2002;80:1699–713.
19. Nardin A, Schrefler B, Lefik M. Application of artificial neural network for identification of parameters of a constitutive law for soils. International Conference on Industrial, Engineering and Other Applications of Applied Intelligent Systems. Springer; 2003. pp. 545–54.
20. Helm D. Pseudoelastic behavior of shape memory alloys: constitutive theory and identification of the material parameters using neural networks. Technische Mechanik-European J Eng Mech. 2005;25:39–58.
21. Chamekh A, Salah HBH, Hambli R. Inverse technique identification of material parameters using finite element and neural network computation. Int J Adv Manuf Technol. 2009;44:173.
22. Landi A, Piaggi P, Laurino M, Menicucci D. Artificial neural networks for nonlinear regression and classification. 10th Int Conf Intell Syst Des Appl. 2010;2010:115–20.
23. Pedregosa F, Varoquaux G, Gramfort A, Michel V, Thirion B, Grisel O, et al. Scikit-learn: machine learning in Python. J Mach Learn Res. 2011;12:2825–30.
24. Chollet F. Keras [Internet]. GitHub; 2015. Available from: https://github.com/fchollet/keras
25. Kingma DP, Ba J, Adam. A Method for Stochastic Optimization. arXiv:14126980 [cs] [Internet]. 2017 [cited 2021 Oct 29]; Available from: http://arxiv.org/abs/1412.6980

26. Awad M, Khanna R. Support Vector Regression. In: Awad M, Khanna R, editors. Efficient Learning Machines: Theories, Concepts, and Applications for Engineers and System Designers [Internet]. Berkeley, CA: Apress; 2015 [cited 2022 Jan 26]. pp. 67–80. Available from: https://doi.org/10.1007/978-1-4302-5990-9_4
27. Rodriguez-Galiano V, Sanchez-Castillo M, Chica-Olmo M, Chica-Rivas M. Machine learning predictive models for mineral prospectivity: an evaluation of neural networks, random forest, regression trees and support vector machines. Ore Geol Rev. 2015;71:804–18.
28. Van Loock G. Predictive value of finite element modelling in design and evaluation of porous lattice structures for orthopaedic implants. [Leuven]: KU LeuvenFaculteit Ingenieurswetenschappen; 2019.
29. Mahnken R, Stein E. A unified approach for parameter identification of inelastic material models in the frame of the finite element method. Comput Methods Appl Mech Eng. 1996;136:225–58.
30. Alomar Z, Concli F. A review of the selective laser melting lattice structures and their numerical models. Adv Eng Mater. 2020;22:2000611.
31. Amani Y, Dancette S, Delroisse P, Simar A, Maire E. Compression behavior of lattice structures produced by selective laser melting: X-ray tomography based experimental and finite element approaches. Acta Mater. 2018;159:395–407.
32. Lozanovski B, Leary M, Tran P, Shidid D, Qian M, Choong P, et al. Computational modelling of strut defects in SLM manufactured lattice structures. Mater Design. 2019;171:107671.
33. Lozanovski B, Downing D, Tran P, Shidid D, Qian M, Choong P, et al. A Monte Carlo simulation-based approach to realistic modelling of additively manufactured lattice structures. Additive Manuf. 2020;32:101092.
34. Gonzalez FJQ, Nuno N. Finite element modeling of manufacturing irregularities of porous materials. Biomaterials Biomech Bioeng. 2016;3:1–14.
35. Hazlehurst K, Wang CJ, Stanford M. Evaluation of the stiffness characteristics of square pore CoCrMo cellular structures manufactured using laser melting technology for potential orthopaedic applications. Mater Design. 2013;51:949–55.
36. Ruiz de Galarreta S, Jeffers JRT, Ghouse S. A validated finite element analysis procedure for porous structures. Mater Design. 2020;189:108546.
37. Li Y, Sang J, Wei X, Yu W, Tian W, Liu GR. Inverse identification of hyperelastic constitutive parameters of skeletal muscles via optimization of AI techniques. Comput Methods Biomech BioMed Eng. 2021;24:1647–59.
38. Fan F, Xiong J, Li M, Wang G. On Interpretability of Artificial Neural Networks: A Survey. arXiv:200102522 [cs, stat] [Internet]. 2021 [cited 2022 Jan 26]; Available from: http://arxiv.org/abs/2001.02522
39. Liu L, Kamm P, García-Moreno F, Banhart J, Pasini D. Elastic and failure response of imperfect three-dimensional metallic lattices: the role of geometric defects induced by selective laser melting. J Mech Phys Solids. 2017;107:160–84.
40. Concli F, Gilioli A. Numerical and experimental assessment of the mechanical properties of 3D printed 18-Ni300 steel trabecular structures produced by selective laser Melting–a lean design approach. Virtual Phys Prototyp. 2019;14:267–76.
41. Zhao M, Zhang DZ, Liu F, Li Z, Ma Z, Ren Z. Mechanical and energy absorption characteristics of additively manufactured functionally graded sheet lattice structures with minimal surfaces. Int J Mech Sci. 2020;167:105262.
42. Jin N, Wang F, Wang Y, Zhang B, Cheng H, Zhang H. Failure and energy absorption characteristics of four lattice structures under dynamic loading. Mater Design. 2019;169:107655.

Publisher's note